

Forward Model and Sensitivity Analysis for Limb-Scattered Radiation of Mesospheric OH Radicals Emission in Ultraviolet Band

FANG Xue-jing^{1,2,3}, XIONG Wei^{1,3*}, SHI Hai-liang^{1,3}, LUO Hai-yan^{1,3}, CHEN Di-hu^{1,3}

1. Anhui Institute of Optics and Fine Mechanics, Hefei Institutes of Physical Science, Chinese Academy of Sciences, Hefei 230031, China
2. University of Science and Technology of China, Hefei 230026, China
3. Key Laboratory of Optical Calibration and Characterization of Chinese Academy of Sciences, Hefei 230031, China

Abstract Hydroxyl, one of the principal oxidants in the atmosphere, determines the density of ozone and other greenhouse gases even the change of climate. In order to achieve high resolution vertical profiles of OH radical in mesosphere, an accurate forward model should be built up for its retrieval. In this paper, this forward model simulates limb-scattered signal including OH solar resonance fluorescence around 309 nm. We calculate OH band rotational emission rate factor g based on molecular spectroscopy theory, and combine it with OH slant column calculated by SCIATRAN to synthesize OH fluorescence emission spectra. By superimposing atmospheric background signal and do a convolution with instrument line shape function, we could obtain a simulated spectra containing OH concentration information. These results are in good agreement with previous measurements by MAHRSI (Middle Atmosphere High-Resolution Spectrograph Investigation) and SHIMMER (Spatial Heterodyne Imager for Mesospheric Radicals). Then we analyze several factors that may influence the forward model. By modifying these parameters, forward model could be more accurate and closer to the actual radiative transfer process in the future.

Keywords OH radical; Forward model; Rotational emission rate factors; SCIATRAN; Sensitivity analysis
中图分类号: O434.2 文献标识码: A DOI: 10.3964/j.issn.1000-0593(2018)10-3278-08

Introduction

The hydroxyl(OH) radical is the most important oxidizing agent in the middle atmosphere, though its mixing ratios are only parts per trillion or billion by volume^[1]. OH chemistry dominates ozone destruction above about 40 km and also serves as a proxy for upper mesospheric water vapor^[2]. Knowing about OH radical will help to understand the atmospheric components and photochemistry events in mesosphere.

Measurements of mesospheric OH have been performed from aircraft, balloons, and satellites^[3-4]. In mid-1990s,

Middle Atmosphere High-Resolution Spectrograph Investigation (MAHRSI)^[1] obtained the first global map of OH in mesosphere. In 2007, Spatial Heterodyne Imager for Mesospheric Radicals (SHIMMER)^[5] measured the solar resonance fluorescence of OH over the diurnal cycle^[3]. It was an instrument that used Spatial Heterodyne Spectroscopy (SHS) technique. Its measurement had a better agreement with standard photochemistry model than that of MAHRSI.

Forward model for MAHRSI was worked out by the basic radiative transfer equation. It considered OH fluorescence, absorption by ozone, Rayleigh scattering by N₂ and O₂ as well as self-absorption. The atmosphere is modeled as a series of

Received: 2017-10-19; **accepted:** 2018-03-08

Foundation item: National Natural Science Foundation of China (11703061), Hefei Institutes of Physical Science Present Foundation (YZJJ201607), Laboratory Innovation Foundation (CXJJ-17S002)

Biography: FANG Xue-jing, (1991—), female, PhD, Anhui Institute of Optics and Fine Mechanics, Hefei Institutes of Physical Science, CAS e-mail: fxj126@mail.ustc.edu.cn *Corresponding author e-mail: frank@aiofm.ac.cn

concentric shells of thickness 2 km. The species density is assumed to be constant within each spherical shell. SHIMMER's forward model for OH is similarly the same when being used for the MAHRSI retrievals.

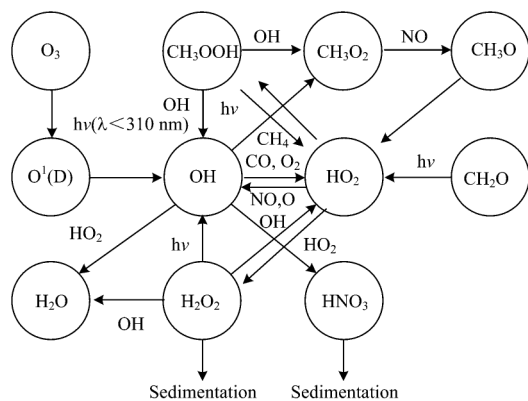


Fig 1 Main OH photochemistry actions in atmosphere

Retrieval is a process to get useful information from measurements. While forward model is the foundation of retrieval. In order to retrieve OH vertical profiles from limb measurements, an accurate and effective forward model is needed. Our work combines basic idea of MAHRSI's forward

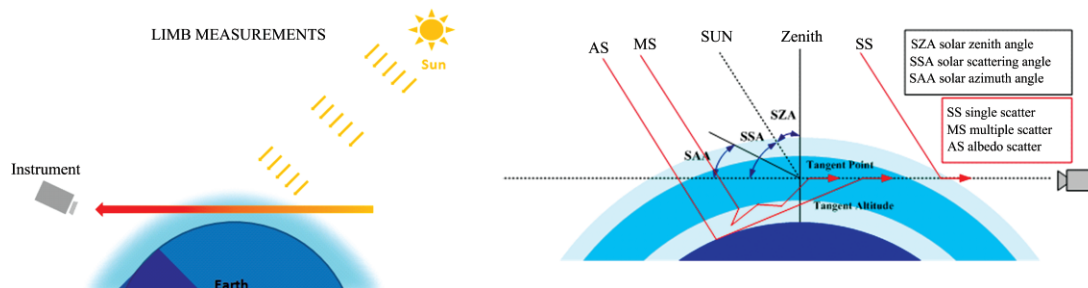


Fig 2 Limb mode geometry

We have built up a modified forward model as is shown in Figure 3, in this forward model, there are three basic components: rotational emission rate factors g , OH slant column along LOS and atmospheric background signal. By synthesizing them together we could obtain a simulated spectrum received by the instrument and OH radiance profiles. The instrument here is a detector used SHS technique which is similar to SHIMMER.

SCIATRAN^[8] covers the spectral range 175.44 nm ~ 4 000 μm comprising the eight spectral channels of the SCIAMACHY (Scanning Imaging Absorption spectroMeter for Atmospheric CHartographY) instrument. SCIATRAN has been developed to perform radiative transfer modeling in any observation geometry appropriate to measurements of the scattered solar radiation in the Earth's atmosphere.

SCIATRAN can build up atmospheric models including 23 kinds of trace gases, Rayleigh scattering, aerosols and

model and convenient radiative transfer model software to make a higher vertical resolution simulation of limb-scattered radiation. In addition, by making use of relatively large electronic cross section of OH around 309 nm^[6], we could work out its fluorescence spectra which is excited by solar energy. This fluorescence signal will be detected together with background signals in limb mode. We will get OH details by analyzing this limb-scattered radiation signal.

1 Forward model

Forward model describes the process that the radiation transfers from the source to the receiver.

The sun is the source in passive remote sensing. As is shown in Figure 2, the solar energy transfers through the atmosphere to the ground, the detector on the track receives limb-scattered signal including information of ingredients in atmosphere, such as trace gases, aerosols and the land surface. In this mode, the line of sight has a long distance and it is more sensitive to trace gas vertical distribution. The price of high vertical resolution is relatively bad horizontal resolution^[7].

clouds. It has stable input parameters and sufficient databases including aerosols, surface reflectance models and suitable ILS (Instrument Line Shape). Above all, it runs quite fast in the retrieval module^[8-10]. The latest version of SCIATRAN is 3. 8. 13, and we use version 3. 3. 2.

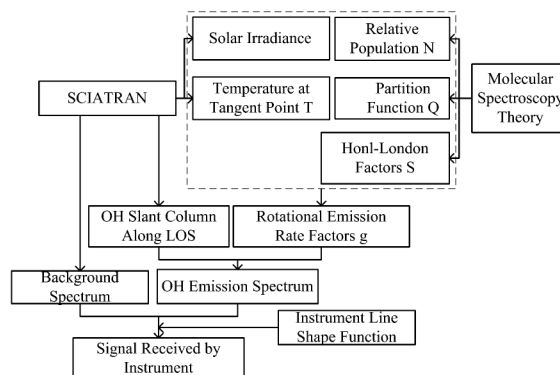


Fig 3 Forward model structure

We complement SCIATRAN's databases to meet our needs, including adding high-resolution NSO (National Solar Observatory) solar spectrum and OH line parameters in ultraviolet band from 'HITRAN on the web' databases.

1.1 Calculation of Rotational Emission Rate Factors *g*

OH radical's solar resonance fluorescence is the excited emergent light by solar radiation around 309 nm. $A^2\Sigma^+$ is the excited state and $X^2\Pi$ is the ground state in $A^2\Sigma^+ - X^2\Pi(0, 0)$ transition. Due to Hund's cases (a) and (b) and Λ doubling of $X^2\Pi^{(1)}$, these two levels split. Following selection rules for this transition, some rotational transitions are allowed in Figure 4^[12].

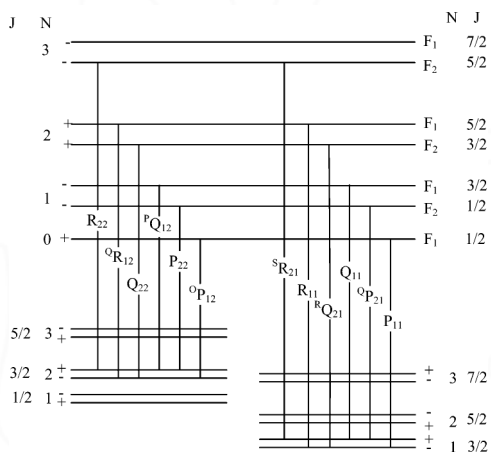


Fig 4 $A^2\Sigma^+ - X^2\Pi(0,0)$ allowed transitions

Rotational emission rate factor *g* measures the emission efficiency of a molecule, which means when being excited by solar radiation, how many photons can emit per second per molecule. Suppose that in mesosphere with thin optical depth, the observed intensity $4\pi I_{\nu'\nu''}$ can be related to the *g* factor^[13],

$$4\pi I_{\nu'\nu''}(z) = \eta(z)g_{\nu'\nu''}(T, z) \quad (1)$$

where $\eta(z)$ is the column abundance along the viewing path and can be calculated by SCIATRAN. The *g* factor is a function of temperature *T* and tangent altitude *z*.

Rotational emission rate factor *g* may be calculated by the expression,

$$g_{\nu'\nu''}(T) = \frac{S(J'J'')}{2J'+1} \omega_{\nu'\nu''} \frac{\pi e^2}{mc^2} f_{\nu'0} \times \sum_{J=|A+\Sigma|}^{\infty} \lambda_{J'J}^3 \pi F_{J'J} \frac{S(J'J)}{2J+1} N_J(T) \quad (2)$$

Where the values of following parameters are the same as that in Stevens and Conway's paper, is the vibrational band branching ratio and $f_{\nu'0}$ is the band oscillator strength. *S* is Hönl-London factors, The branching ratios $\omega_{00} = A_{00}/\Sigma A_{0\nu'}$ taken to be 1.00. The constant $\frac{\pi e^2}{mc^2} = 8.829 \times 10^{-20} \text{ cm}^2 \cdot \text{nm}^{-1}$ and the absorption oscillator strength $f_{00} = 1.04 \times$

10^{-3} . λ is the wavelength of the absorption transitions. πF (photons/cm²/s/nm) used in [Stevens and Conway 1999] is the unattenuated solar irradiance at the top of the atmosphere. We modify it by considering the extinction from the sun to the tangent point, though the optical thickness is relatively small between 45km-85km. The extinction process is calculated by SCIATRAN.

There are other parameters need to be calculated using molecular spectroscopy theory, HITRAN databases^[14], energy level information J' , J'' and low energy E_0 . $N_J(T)$ is the relative population in rotational level *J* at temperature *T*. It could be calculated by Boltzmann distribution.

If the hydroxyl molecules in the atmosphere are in thermal equilibrium, the rotational population distribution can be described by the Maxwell-Boltzmann distribution law^[6,15-16].

$$N(\nu, \nu', J, J', T) = \frac{(2J+1)\exp(-hcE(J)/kT)}{Q(T)} \quad (3)$$

where *h* is Plank's constant, *c* is the speed of light, $E(J)$ (cm⁻¹) is the energy of the $X^2\Pi$ state, *k* is the Boltzmann constant, *T* is the equilibrium temperature in *K*, and $Q(T)$ is the partition function. The partition function $Q(T) = Q_v Q_r$, where the vibrational partition function Q_v is

$$Q_v = (1 - \exp[-hc\omega_e/kT])^{-1} \quad (4)$$

ω_e is the first order vibrational constant which is equal to 3737.761 cm⁻¹. Because of this large energy separation between vibrational levels, $Q_v \approx 1$ at middle atmospheric temperatures.

The rotational partition function Q_r is

$$Q_r = \sum_{J'', \Sigma''} (2J''+1)\exp(-hcE(J'', \Sigma'')/kT) \quad (5)$$

Thus, $N_J(T)$ is worked out as is showed in Figure 5.

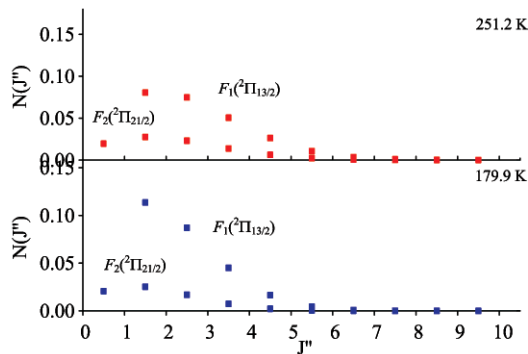


Fig 5 Calculated relative population of the ground rotational states of OH

Solar irradiance showed in Figure 6 with a high spectral resolution of $3.5 \times 10^{-4} \text{ nm}$ in this band (308.2~309.8 nm) used in this calculation is from NSO (National Solar Observatory)^[17] and it has already been modified so that it's the direct irradiance at the observation point.

The *g* factors results compared with Stevens and Conw-

ay's work is shown in Figure 7. We choose the temperature 200K because the previous works have published a result at this temperature which is nearly the temperature at 70 km in mesosphere. We can tell that our results are about 60% larger because of the larger solar irradiance. And change of HIT-RAN databases of OH molecule in these years may cause different relative intensity.

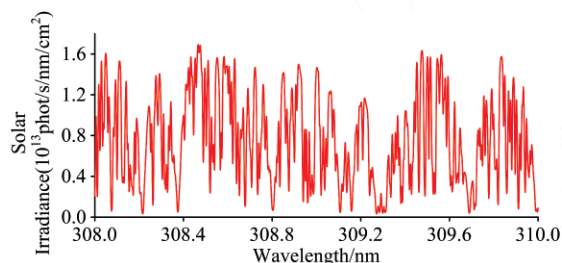


Fig 6 Solar irradiance used in calculation of g factors

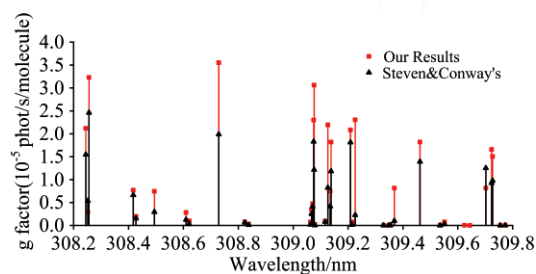


Fig 7 g factors calculation comparison with previous work at 200 K

1.2 Slant column and Background

We use the profiles of OH, O_3 and other trace gases in SCIATRAN B2D profiles databases to match the forward model algorithm of SCIATRAN. In forward model simulation, we calculate 45 km to 85 km in 1 km step.

Slant column is the column abundance along the viewing path, which could be calculated by the absorption of OH along the LOS. Thus the final signal may include the OH abundance information which can be retrieved from formula (1).

The limb mode has a long viewing path which leads to a relatively large slant column. Under optically thin condition, the emission energy may transfer from the observation point to the instrument without attenuation. The slant column in 70 km tangent point calculated by SCIATRAN with parameter settings listed in Table 1 is showed in Figure 8. Each wavelength has different value because the algorithm used in slant column calculation depends on the absorption characteristics of OH. This may mean that stronger absorption line corresponds to relatively larger slant column and the integration over the band should be equal to column abundance in unit molecules \cdot cm^{-2} . The spectral band we choose is 308.2 ~ 309.8 nm which meets the need of our spatial heterodyne

spectrometer that intends to detect mesospheric OH radicals. At the same time, we calculate solar direct radiance at each tangent point.

Table 1 Main input parameters settings in SCIATRAN

Input parameters	Value
Spectral segment information/nm	308.2~309.8, 0.001
Trace gases	BrO, NO_3 , OClO, O_3 , NO_2 , SO_2 , ClO, HCHO, OH, HF, HCl
Tangent height/km	45~85
Solar zenith angle/($^\circ$)	50
Solar azimuth angle/($^\circ$)	120
Surface settings	Lambertian; soil
Aerosol settings	LOWTRAN aerosol

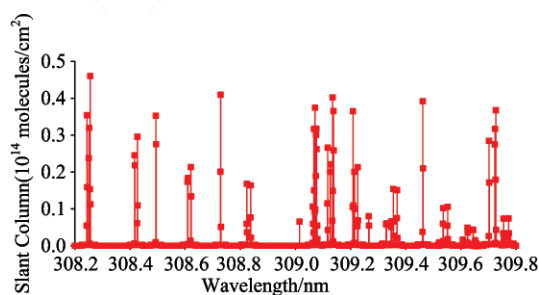


Fig 8 Calculated slant column at 70 km for each wavelength

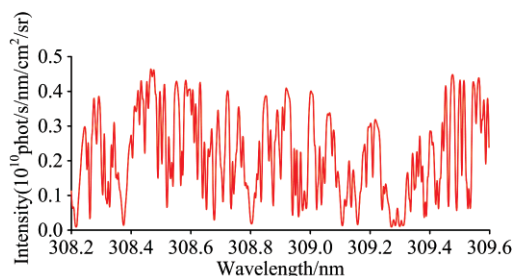


Fig 9 Calculated background signal

Figure 9 shows simulated background spectrum in 70 km with the same settings in slant column calculation. The shape is almost like the solar irradiance because it consists of Rayleigh scattering, extinction of OH itself, aerosols and other trace gases without OH emissions, whose value depends on atmospheric condition including solar irradiance, aerosol, cloud, trace gases, surface and observation geometry. In this case, we don't consider cloud due to its ignorable disturbance in mesospheric limb mode.

We add the product of g factors and slant column to the background signal, then do a convolution with the instrument line shape function which is a Gaussian function with a FWHM of 0.015 nm. This FWHM value corresponds to the spectral resolution of our spatial heterodyne spectrometer.

Using this forward model, we also simulate OH emission signals at different altitudes between 45 and 85 km. The OH intensity increases as the height goes down, but combining Figure 10 and Figure 11, we can tell that at 40 km, OH signal is difficult to be distinguished from the total signal because of rapid increasing of Rayleigh scattering signal in lower altitudes.

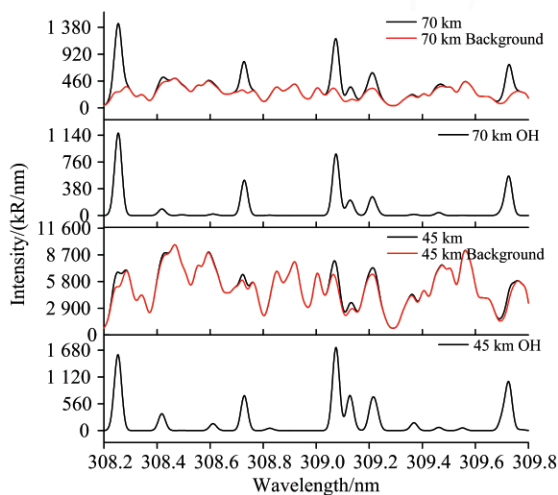


Fig 10 Simulated results at 45 and 70 km. In upper two panels are the synthetic signal, background signal and the OH emission signal at 70 km. In lower two panels are ones at a different tangent height of 45 km

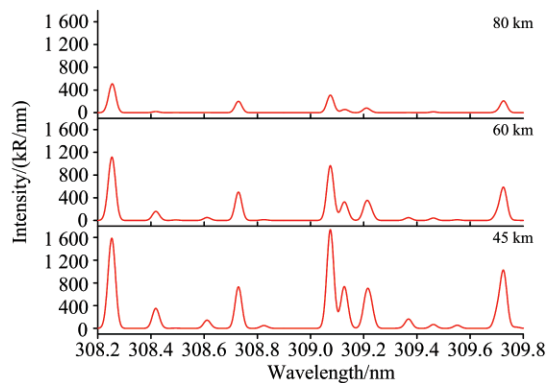


Fig 11 OH emission intensity in different tangent height

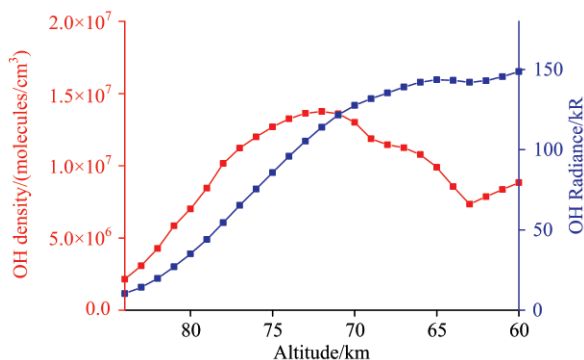


Fig 12 Input OH density profile and simulated OH radiance

Figure 12 shows OH density and radiance profiles between 60 and 85 km. We choose this altitude range for analyzing because our forward model is more applicable and accurate in this area and previous research such as SHIMMER has a reliable result only in this range. From this result we can tell that the intensity of OH emission signal is related to the density at different tangent heights. The shape of the OH radiance profile is similar to that of density profile.

2 Sensitivity Analysis

There are some important parameters in forward model which would have an effect on the results, which would even influence the retrieval accuracy. Geometric parameters, aerosols and OH concentration are considered in this sensitivity analysis. Default settings are listed as in Table 1.

2.1 Geometric parameters

In the mesosphere, land surface parameters are relatively small, so the most important factors in limb observation mode is the geometry parameters including solar zenith angle, solar azimuth angle and tangent point position. These three parameters determine the position of the observation point.

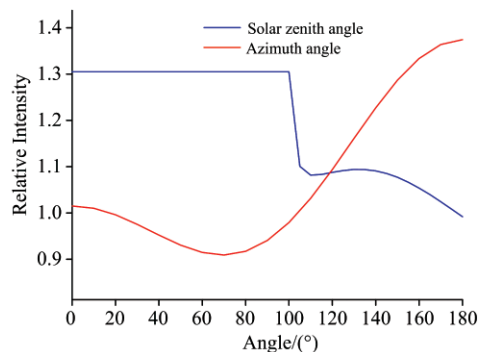


Fig 13 Observation radiance with different solar zenith angles and azimuth angles

The parameter of “Azimuth angles” here defines the values of the relative azimuth angles of line-of-sight with respect to the sun. The value of 0° means instrument is pointed into the solar direction. The intensity decreases rapidly with increasing SZA near 90° because in this position, the observation geometry is going into twilight mode like in Figure 14 (b). In azimuth angles sensitivity analysis, when $SAA = 180^\circ$, the sun and the instrument are in a line by two sides, so more transmitted and scattered solar radiation are transferred into the instrument.

2.2 Aerosol

The sum of the aerosol scattering coefficient and the aerosol absorption coefficient yields the aerosol extinction coefficient for each aerosol type. These three coefficients have the unit of an inverse length (km^{-1}).

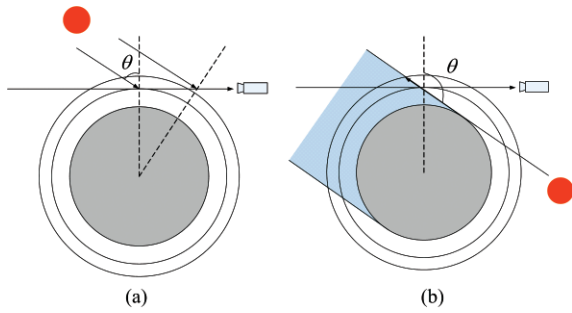


Fig 14 Geometry in (a) nontwilight (b) twilight

We use user-define aerosol settings and set AOT in range of 0 to 5 by the step of 0.05 with reference wavelength of 308 nm. For mesospheric aerosol, scattering coefficient is much larger than absorption coefficient^[6]. Therefore, larger AOT brings out larger limb-scattered radiation. Figure 15 proved this statement.

2.3 OH concentration

We do a 10% perturbation to OH concentration by step of 1 km and simulate limb-scattered radiance in 41 tangent heights between 44 to 84 km.

The relationship between limb-scattered radiance and OH concentration could be described by a parameter called

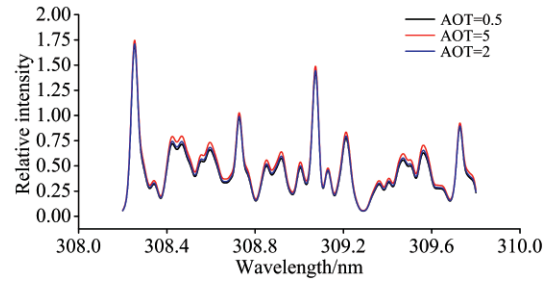


Fig 15 Limb-scattered radiance at 70 km with different AOT

“Weighting Functions”. It’s a matrix usually used in retrieval, whose element could be expressed as

$$K_{jk} = \frac{\partial I_j}{\partial n_k} = \frac{\Delta I_j}{\Delta n_k}$$

Where I_j is the limb-scattered radiance and n_k is the OH concentration in the tangent height j , Δ is the difference before and after perturbation.

From Figure 16, we can tell the sensitive tangent height range for OH is above 70 km. That is to say, it’s more effective and would have higher accuracy of OH’s retrieval in this height. The weighting function has different maximum intensity in different wavelength due to relative intensity of OH emission line.

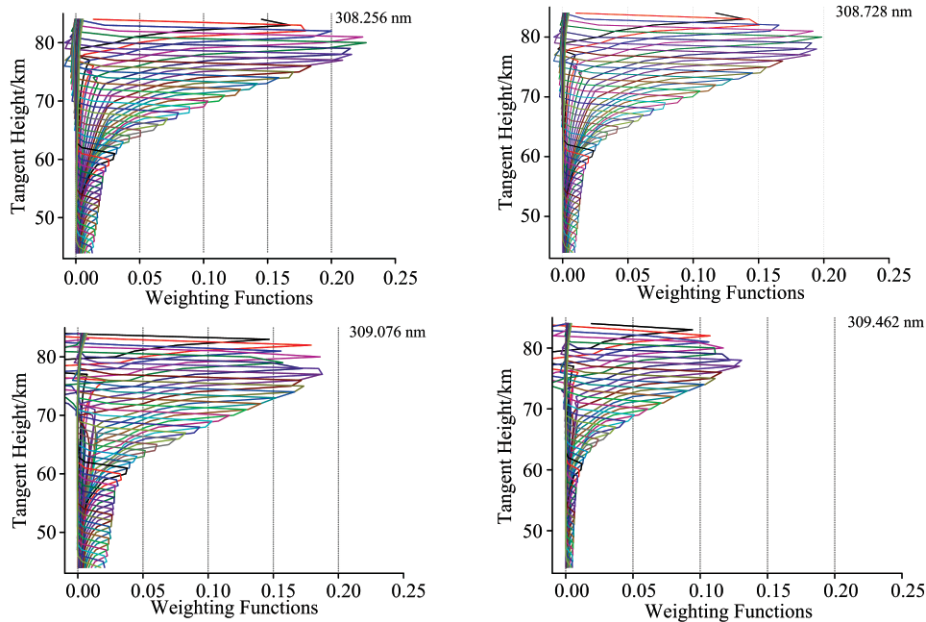


Fig 16 OH Weighting functions in different wavelength

3 Discussions

(1) Factors in g factor calculation

Formula (1) is applicable under optically thin conditions and in absence of quenching. If atmospheric optical thickness could not be neglected, the results using this formula may not

be accurate. That is to say, the effective range for this algorithm is at least 50 km above. The higher the altitude is, the more accurate the forward model is. In lower altitude, the air is becoming thicker, more N_2 and O_2 may influence the stability of OH excited state. In another way, the background signal may become too large to distinguish OH signal from it.

We can see that in formula (2) there are so many param-

eters in calculating g factor. Solar irradiance and temperature are the two most important factors in this calculation, which need to be as accurate as possible for this model.

(2) Factors in SCIATRAN simulation

There are common errors in forward model which are the differences between the input conditions and the actual conditions. The analysis should be discussed by combining measurements and retrieval results. In this case, we definitely should build forward model as close as to the actual situation to reduce the retrieval uncertainty and errors.

(3) Sensitivity analysis

In limb mode in mesosphere, features of land surface wouldn't matter a lot for scattered signal. And thinner optical condition may lead to less extinction of intensity. Measurement of OH in mesosphere is seemed to be influenced by the OH concentration itself and long viewing path. OH density profile peaks at about 70 km and the background signal is rather small, so it's easier to separate OH signal from Rayleigh scattered signal. Accuracy of forward model and retrieval depend on these atmospheric parameter settings definitely. We would make a detailed analysis in future works which focus on clouds or other trace gases such as ozone.

4 Conclusion

We calculate OH band rotational emission rate factors g

based on molecular spectroscopy theory. What's more, combining with solar irradiance and slant column calculated by SCIATRAN, we obtain the simulated received signals by the spatial heterodyne spectrometer at 50~80 km. This spectrum contains OH concentration information along the viewing path. By using an effective retrieval algorithm, OH density at each altitude could be worked out using this forward model. Sensitivity analysis of several atmospheric parameters is also done to give a brief understanding of components which have effects in radiative transfer model. It is important to build an accurate forward model, especially for OH radicals in the order of magnitude of ppbv. This forward model provides a foundation for retrieving atmospheric OH radical in high precision and also much valuable information for researching on the mesospheric photochemical processes.

Acknowledgements

The authors of this study would like to thank Key Laboratory of Optical Calibration and Characterization of Chinese Academy of Sciences for funding this research. We would like to thank Dr. Alex Rozanov from Institute of Environmental Physics/Institute of Remote Sensing, University of Bremen, Germany for helpful advices in using SCIATRAN.

References

- [1] Conway R R, Stevens M H, Brown C M, et al. *Journal of Geophysical Research*, 1999, 104(D13): 16327.
- [2] Summers M E, et al. *Geophysical Research Letters*, 2001, 28(18): 3601.
- [3] Englert C R, Stevens M H, et al. *Geophysical Research Letters*, 2008, 35: L19813.
- [4] Zhao W, Wysocki G, et al. *Optics Express*, 2011, 19: 2493.
- [5] Englert C R, Stevens M H, et al. *Journal of Geophysical Research*, 2010, 115: D20306.
- [6] Fennelly J A, Torr D G, Torr M R. *Journal of Geophysical Research*, 1989, 94: 5183.
- [7] Kaiser J W. *Atmospheric Parameter Retrieval from UV-Vis-NIR Limb Scattering Measurements*. Bremen: University of Bremen, 2001.
- [8] Rozanov V V, Buchwitz M, et al. *Advances in Space Research*, 2002, 29(11): 1831.
- [9] Rozanov A, Rozanov V, Buchwitz M, et al. *Advances in Space Research*, 2005, 36: 1015.
- [10] Rozanov V V, Rozanov A V. *User's Guide for the Software Package SCIATRAN-Version 3.2*. Institute of Remote Sensing, University of Bremen, Germany, 2013.
- [11] Herzberg G. *Spectra of Diatomic Molecules*. Van Nostrand Reinhold, New York, 1950.
- [12] Anderson J G. *Journal of Geophysical Research*, 1971a, 76: 4634.
- [13] Stevens M H, Conway R R. *Journal of Geophysical Research*, 1999, 104: 16369.
- [14] HITRAN on the web-<http://hitran.iao.ru>.
- [15] Goldman A, Gills J R. *Journal of Quantitative Spectroscopy Radiative Transfer*, 1981, 25: 111.
- [16] Cageao R P, Ha Y L, et al. *Journal of Quantitative Spectroscopy Radiative Transfer*, 1997, 57: 703.
- [17] National Solar Observatory-<http://vso.nso.edu>.

中高层 OH 自由基在紫外波段的临边散射辐射正演模拟与敏感性分析

方雪静^{1,2,3}, 熊伟^{1,3*}, 施海亮^{1,3}, 罗海燕^{1,3}, 陈迪虎^{1,3}

1. 中国科学院合肥物质科学研究院安徽光学精密机械研究所, 安徽 合肥 230031
2. 中国科学技术大学, 安徽 合肥 230026
3. 中国科学院通用光学定标与表征技术重点实验室, 安徽 合肥 230031

摘要 OH 自由基是中高层大气中重要的氧化剂, 决定着臭氧以及其他温室气体的浓度变化, 甚至气候变化。为了实现中高层大气 OH 自由基的精细探测与精确反演, 需要构造正演模型, 模拟得到仪器接收到的大气中的 $A^2\Sigma^+ - X^2\Pi(0,0)$ 309 nm 波段的太阳共振荧光发射信号。本文基于分子光谱能级跃迁理论计算得到 OH(0,0) 振动能级上的荧光发射率因子 g , 结合辐射传输模型 SCIATRAN 模拟出的太阳辐照度和观测视线路径上的 OH 柱量, 模拟出 OH 荧光发射光谱, 叠加上大气背景光谱并卷积仪器函数, 最终模拟得到仪器接收的包含 OH 浓度信息的光谱。模拟结果与国外在轨仪器 MAHRSI (Middle Atmosphere High-Resolution Spectrograph Investigation), SHIMMER (Spatial Heterodyne Imager for Mesospheric Radicals) 的在轨实测结果一致性较好。还分析了影响模拟结果的因素, 在之后的正演过程中加以修正, 使正演模型更接近实际辐射传输过程。

关键词 OH 自由基; 正演模型; 荧光发射率因子; SCIATRAN; 敏感性分析

(收稿日期: 2017-10-19, 修订日期: 2018-03-08)

* 通讯联系人

